A Broadband Dual-Polarized Printed Antenna

Ruina Lian[*], Shao-Shuai Zhang, Ying-Zeng Yin, Xue-Yan Song, and Hao Zhang

Abstract—A low-profile broadband dual-polarized antenna with high isolation and low cross polarization is presented in this letter. The proposed antenna employs two different feeding mechanisms. On one hand, two out-of-phase probes loaded with two small circular patches make the proposed antenna operate in horizontal mode. On the other hand, two pins connecting two eyebrow-shaped patches and the ground form a magnetic loop which enables the proposed antenna to achieve vertical polarization. By elaborately adjusting the feeding structures, measurements demonstrate that the proposed antenna not only achieves 10-dB return loss bandwidths of 49% (1.7–2.8 GHz) and 28% (2–2.65 GHz) for port 1 and port 2, respectively, but also maintains a high isolation better than 32 dB over the entire common frequency band. Meanwhile, within the main lobes, the cross polarization levels, both in E-plane and in H-plane, stay lower than -25 dB for port 1 and -20 dB for port 2. In addition, the proposed antenna with a profile of $0.13\lambda_0$ achieves the maximum gains of 8.4 dBi for horizontal polarization and 8.2 dBi for vertical polarization.

1. INTRODUCTION

Dual-polarized antenna is gaining ever increasing interest recently, owing to its abilities to mitigate the multipath fading problem and increase channel capacity. Moreover, it could also be employed as dual-polarized multiple-input-multiple-output (MIMO) antennas, instead of two spatially separated antennas with single polarization [1–3]. In modern communication systems, antennas with polarization diversity are highly desired. For a dual-polarized antenna to work effectively, high isolation, low cross-polarization level and stable gain are demanded. Actually, there exists great difficulty in achieving all these performances simultaneously. Many studies have been performed to design favorable dual-polarized antennas. As shown in [4–6], stacked patches, as a classical antenna type, could achieve dual polarizations with the aid of aperture coupling. In the open literature [7], an antenna fed by two different feeding methods achieves high isolation and low cross polarization. However, its bandwidth is only 14%. Though another antenna in [8] achieving dual polarizations by exploiting the even and odd modes of a CPW structure has a wide bandwidth, it cannot avoid high cross polarization.

In this paper, we present a new design for a broadband dual-polarized printed antenna fed by two different input ports (See Figure 1): port 1 belonging to electrical feed and port 2 being attributed to magnetic feed. The electro-magnetically feeding structures mounted orthogonally are introduced to form a dual-polarized antenna with wide bandwidth and high isolation. Due to the two out-of-phase probe feeds located in the same resonant direction and at symmetric positions with respect to the patch center, some unwanted higher order modes that contribute to polarization impurity can be suppressed [9, 10]. As expected, the proposed antenna keeps low cross-polarization levels within the main lobes across the entire common frequency band.
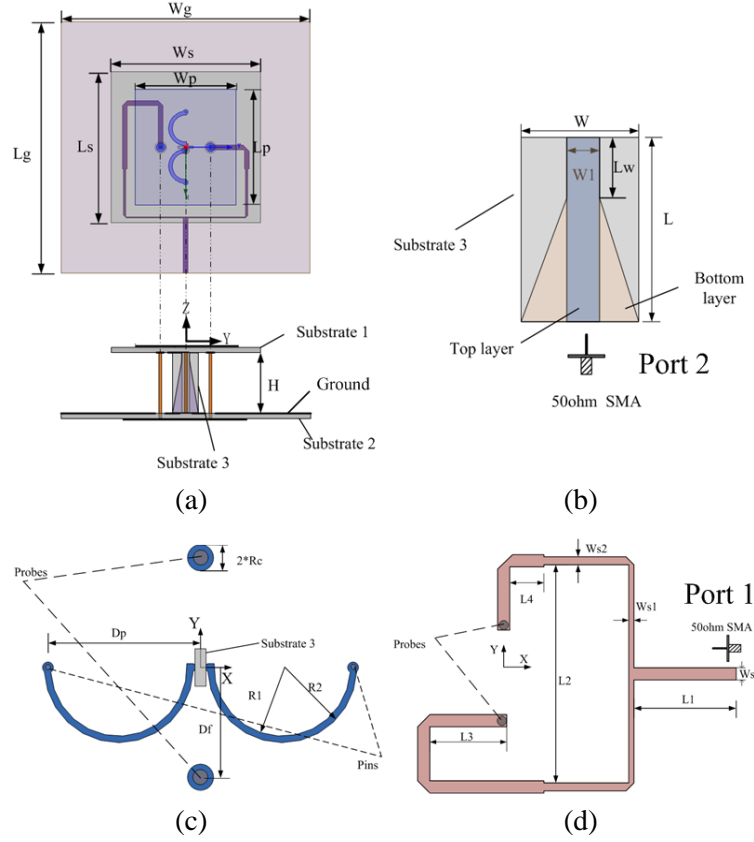
Figure 1. Geometry of the proposed antenna: (a) top and side view, (b) balun, (c) detailed show, and (d) divider. Some of the optimized key parameters are listed as follows: $W_g = L_g = 100$, $W_s = L_s = 60$, $W_p = 40.5$, $L_p = 46$, $W = 6$, $L = 15$, $W_1 = 2$, $L_w = 3$, $H = 15$, $D_p = 14$, $D_f = 10$, $R_1 = 6.25$, $R_2 = 6.85$, $R_c = 1.2$, $W_s = 1.9$, $W_{s1} = 0.4$, $W_{s2} = 1$, $L_1 = 22$, $L_2 = 48$, $L_3 = 12.6$, $L_4 = 7.7$ (Units: mm). The radii of the probe and the pin are 0.65 mm and 0.35 mm, respectively.

2. ANTENNA CONFIGURATION AND DESIGN

The proposed antenna whose profile is $0.13\lambda_0$ (λ_0 is the free space wavelength at the center frequency), as shown in Figure 1, has a rectangular radiating patch with an area of 46 mm × 40.5 mm printed on the top of substrate 1. Besides the patch, the proposed antenna is basically made up of electro-magnetically feeding mechanisms. Firstly, two out-of-phase probes directly connect with two small circular patches with the same radius of 1.2 mm, which then couple the energy to the rectangular radiating patch. This forms electrically-fed antenna. The rectangular radiating patch and the small circular patch located on the bottom of substrate 1 can produce an appropriate capacitance for counteracting the inductance caused by the long probe so as to achieve a sufficiently wide operating band. A divider (as illustrated in Figure 1(d)) makes the two probes differ $180°$ in phase so that the proposed antenna maintains low cross polarization level. Secondly, two eyebrow-shaped patches, which are also symmetrically printed on the bottom of substrate 1, are connected to the ground by two pins, thus forming a magnetic loop. Moreover, as shown in Figure 1(c), the two eyebrow-shaped patches are separated by a gap where a balun (See Figure 1(b)) is located. When excited, such a magnetic loop will also couple the energy to the rectangular radiating patch. This forms magnetically-fed antenna. These two different feeding structures are orthogonally located with respect to the center of the antenna, thus shaping the broadband dual-polarized printed antenna. In addition, the proposed antenna has three 1-mm-thick FR4 substrates, all of which possess the dielectric constant (ε_r) of 4.4 and the loss tangent ($\tan\delta$) of 0.02.

3. SIMULATION AND MEASUREMENT RESULTS

In order to have an insight into the influence of different parameters on the antenna, simulations have been conducted by HFSS 13.0. In the following discussion, when one parameter varies, the others stay invariable. To verify the design, a prototype of the proposed antenna with the finally optimized parameters has been built and measured. Figure 2 shows photographs of the proposed antenna.

3.1. Analysis of S-Parameters

The measured and simulated S-parameters for the two feeding ports of the proposed antenna are depicted in Figure 3. The measured impedance bandwidths, determined by -10 dB, are 49% (1.7–2.8 GHz) and 28% (2–2.65 GHz) while the simulated impedance bandwidths are 43.5% (1.8–2.8 GHz) and 26.5% (2–2.61 GHz) for port 1 and port 2, respectively. Besides a wide common frequency band, the proposed antenna also achieves a better isolation higher than 32 dB between the two ports over the entire common bandwidth. As seen from Figure 3, good agreement lies between the simulated and measured S-parameters, including the reflection coefficient and isolation. The slight discrepancy may be contributed to the error in fabrication due to the slender and soft pins.

In the process of designing the proposed antenna, the radius R_c of the small circular patch and width W_p of the rectangular radiating patch are the key parameters having significant influence on the impedance match for port 1. In what follows, the simulated $|S_{11}|$ with different R_c and different W_p are plotted in Figure 4 and Figure 5, respectively. As shown in Figure 4, the size of the small circular patch affects all the three resonances. With an increase in the value of R_c, the first and the third resonances move together towards the lower frequency while the second resonance makes an inverse change, which

(a)　　　　　　　　(b)　　　　　　　　(c)
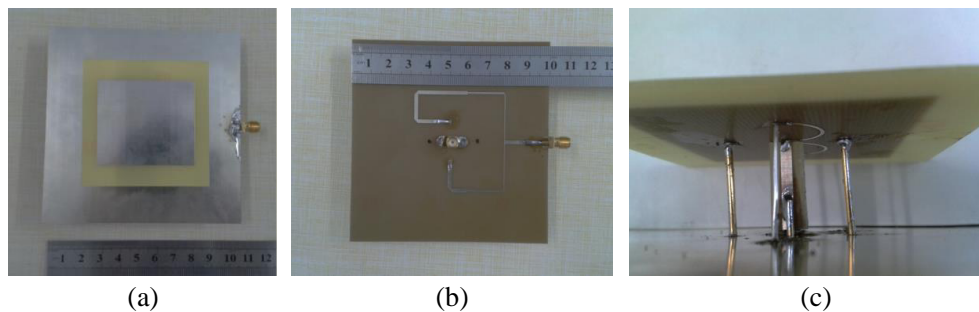
Figure 2. Photographs of the proposed antenna: (a) top view, (b) bottom view, and (c) detailed show.
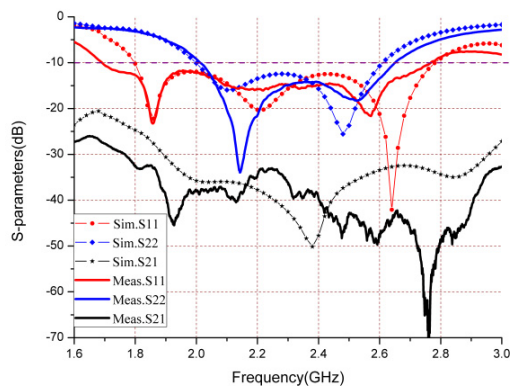
Figure 3. Simulated and measured S-parameters of the proposed antenna.
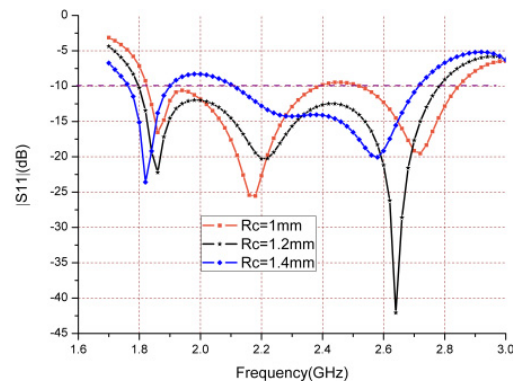
Figure 4. simulated $|S_{11}|$ of the proposed antenna with different R_c.

will make the second resonance merge with the third one, thus narrowing the working bandwidth. It is apparent that when R_c equals 1.2 mm, the impedance match reaches its best condition, and either smaller or bigger value will lead to bad performance. See Figure 5, when W_p is enlarged, the first resonance keeps invariant and however, the second and the third ones march together towards the lower frequency. In such a case, the first resonance will unite with the second one sooner or later. For a wide operating bandwidth, a proper value 40.5 mm is selected for the width of the rectangular patch.
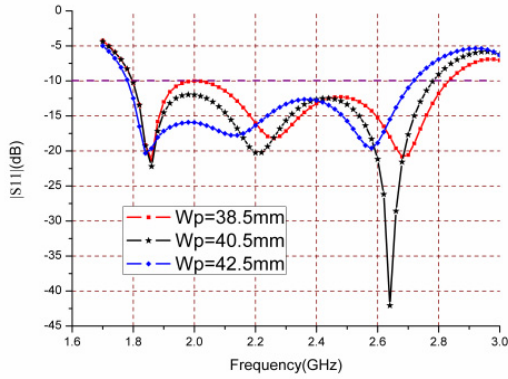
Figure 5. Simulated $|S_{11}|$ of the proposed antenna with different W_p.
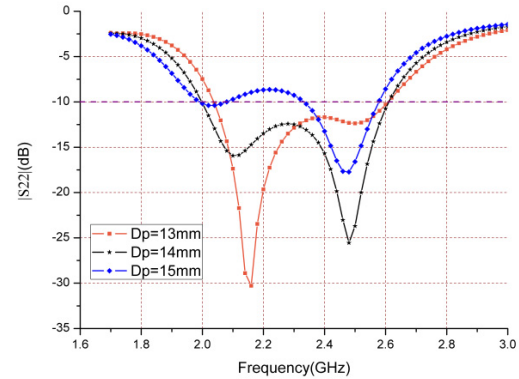
Figure 6. Simulated $|S_{22}|$ of the proposed antenna with different D_p.
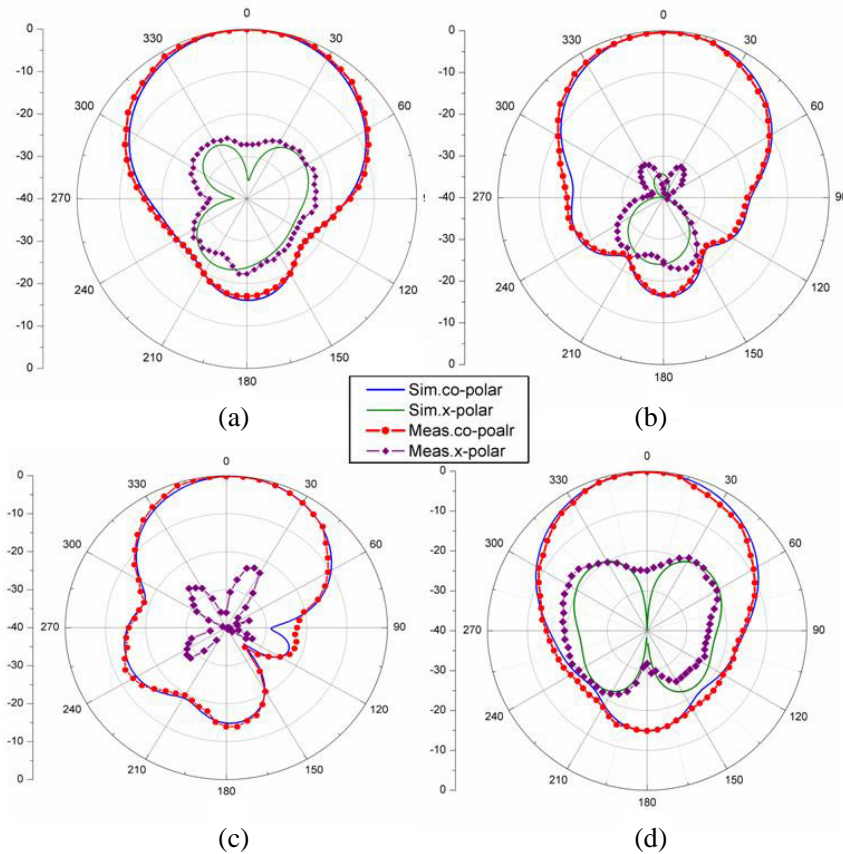
Figure 7. Measured and simulated radiation patterns at 2.2 GHz for port 1, (a) H-plane and (b) E-plane and port 2 (c) E-plane and (d) H-plane.

As for port 2, the distance D_p of the short pin from the patch center and the radius of the short pin are the very parameters determining the impedance match condition. For brief, the influence of different pin's radii on $|S_{22}|$ is not given out. Figure 6 illustrates the simulated $|S_{22}|$ of the proposed antenna with different D_p. Obviously, let D_p equal 14 mm, the proposed antenna has the maximum bandwidth and good impedance match.

3.2. Analysis of Radiation Patterns

The radiation patterns of the proposed antenna for both polarization modes are measured in an anechoic chamber. Port 2 is terminated with a 50-ohm load when the radiation pattern of port 1 is being tested, and vice versa. As illustrated in Figures 7 and 8, the measured and simulated radiation patterns of the proposed antenna at frequencies of 2.2 GHz and 2.4 GHz for both polarization modes agree very well except for the cross polarization patterns. It can be seen that the main beam of the radiation always lies towards the broadside z-direction without any tilt. Both in E-plane and in H-plane, the detailed cross polarization levels within the main lobes for the two ports are listed in Table 1. The front-to-back ratios

Table 1. Cross polarization levels of the proposed antenna.

Port Frequency	port 1 (dB)		port 2 (dB)	
	E-plane	H-plane	E-plane	H-plane
2.2 GHz	≤ -30	≤ -25	≤ -22	≤ -20
2.4 GHz	≤ -30	≤ -30	≤ -30	≤ -20

Table 2. 3-dB beam widths of the proposed antenna.

Port Frequency	port 1		port 2	
	E-plane	H-plane	E-plane	H-plane
2.2 GHz	64.9°	72.8°	62.2°	73.5°
2.4 GHz	60°	68.6°	58.5°	68°
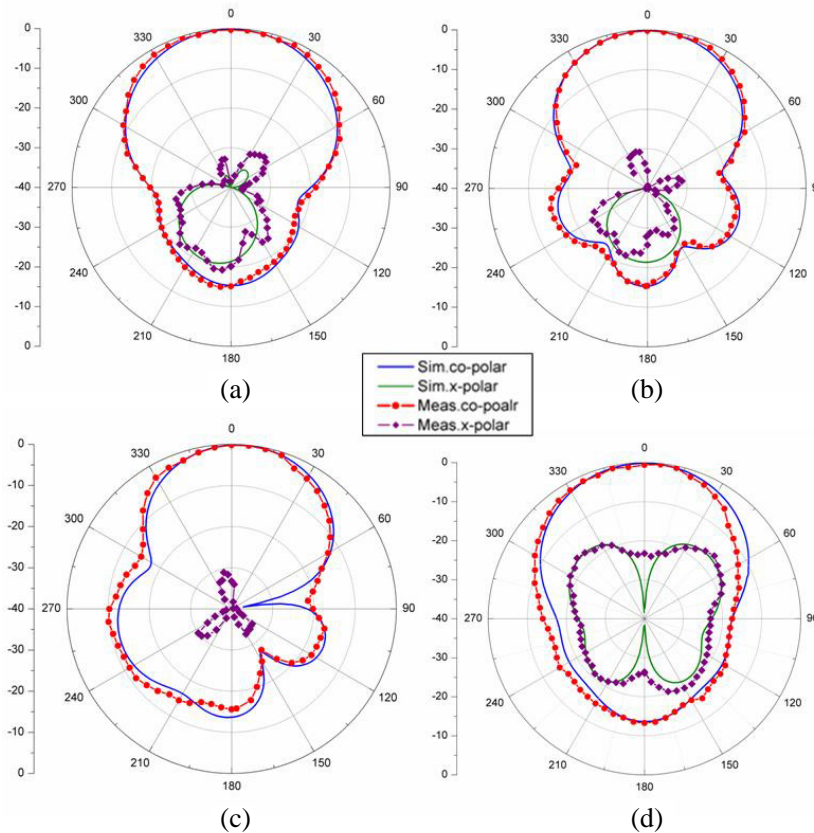
Figure 8. Measured and simulated radiation patterns at 2.4 GHz for port 1 (a) H-plane and (b) E-plane and port 2 (c) E-plane and (d) H-plane.

remain over 15 dB and 13 dB for port 1 and port 2, respectively, due to the small metalized ground. See Table 2, the 3-dB beam widths are also exhibited in detail.

3.3. Analysis of Gains

The measured and simulated gains for port 1 and port 2 are plotted in Figure 9. As indicated, the measured curves coincide with the simulated ones. The gain difference between the two polarizations is mainly ascribed to the two different feeding mechanisms. Over the entire common operating frequency band, the proposed antenna achieves stale and high gains ranging from 6.5 dBi to 8.4 dBi for port 1 and from 7.5 dBi to 8.2 dBi for port 2.

3.4. A Thorough Comparison

To compare some of the recent work in wideband dual-polarized patch antenna with the proposed one, Table 3 lists the features in terms of profile, common bandwidth, port isolation and cross polarization levels within main lobes across the entire common frequency band. As observed in the table, there are some antennas with low profile and high isolation but the bandwidths seem not enough. Also, there are some antennas with good performance including wide bandwidth, high isolation and low cross polarization but the profiles seem high. Through the thorough comparison, the proposed antenna exhibits relatively good performance which enables it to be potential in the wireless communication.
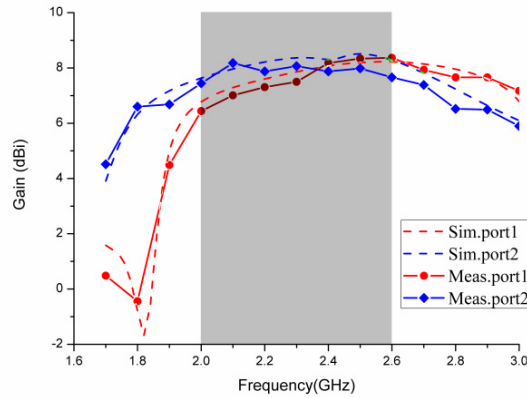
Figure 9. Measured and simulated gains for the proposed antenna.

Table 3. comparison between antennas in references and the proposed one.

Antennas	Profile	Common Bandwidth	Isolation (dB)	Cross Polarization (dB)	
				port 1	port 2
Antenna in [11]	negligible	400%	≥ 20	≤ -5	≤ -5
Antenna in [12]	$0.08\lambda_0$	11%	≥ 20	≤ -10	≤ -15
Antenna in [13]	$0.15\lambda_0$	29%	≥ 30	≤ -15	≤ -15
Antenna in [14]	$0.1\lambda_0$	19%	≥ 28	≤ -15	≤ -15
Antenna in [15]	$0.19\lambda_0$	29%	≥ 23	≤ -20	≤ -25
Antenna in [16]	$0.15\lambda_0$	24.9%	≥ 29	≤ -15	≤ -20
Antenna in [17]	$0.18\lambda_0$	26%	≥ 25	≤ -15	≤ -18
Proposed antenna	$0.13\lambda_0$	28%	≥ 32	≤ -20	≤ -25

4. CONCLUSION

In this letter, a low-profile wideband dual-polarized antenna with high isolation and low cross polarization is designed by properly adopting electromagnetically feeding structures. The prototype is built and measured, which achieves a common frequency band from 2.0 GHz to 2.65 GHz for both polarizations. Over the entire common operating frequency band, the isolation between the two ports keeps higher than 32 dB while the cross polarization levels stay lower than -25 dB for port 1 and -20 dB for port 2 within the main lobes. Moreover, in both the horizontal and vertical modes, the proposed antenna obtains relatively high and stable gains. With the good performance, the proposed antenna will easily find its applications in modern communication systems.

REFERENCES

1. Brown, T., "Indoor MIMO measurements using polarization at the mobile," *IEEE Antennas Wireless Propag. Lett.*, Vol. 7, 400–403, 2008.

2. Landon, D. and C. Furse, "Recovering handset diversity and MIMO capacity with polarization-agile antennas," *IEEE Trans. Antennas Propag.*, Vol. 55, No. 11, 3333–3340, 2007.

3. Konanur, A., K. Gosalia, S. Krishnamurthy, B. Hughes, and G. Lazzi, "Increasing wireless channel capacity through MIMO systems employing co-located antennas," *IEEE Trans. Microw. Theory Tech.*, Vol. 53, No. 6, 1837–1844, 2005.

4. Gao, S. C., L. W. Li, P. Gardner, and P. S. Hall, "Wideband dual-polarised microstrip patch antenna," *Electronics Lett.*, Vol. 37, No. 20, 1213–1214, 2001.

5. Gao, S.-C., L.-W. Li, M.-S. Leong, and T.-S. Yeo, "Dual-polarized slot-coupled planar antenna with wide bandwidth," *IEEE Trans. Antennas Propag.*, Vol. 51, No. 3, 441–448, 2003.

6. Gao, S., L. W. Li, M. S. Leong, and T. S. Yeo, "A broad-band dual-polarized microstrip patch antenna with aperture coupling," *IEEE Trans. Antennas Propag.*, Vol. 51, No. 4, 898–900, 2003.

7. Chiou, T.-W. and K.-L. Wong, "Broad-band dual-polarized single microstrip patch antenna with high isolation and low cross polarization," *IEEE Trans. Antennas Propag.*, Vol. 50, No. 3, 399–401, 2002.

8. Li, Y., Z. Zhang, W. Chen, Z. Feng, and M. F. Iskander, "A dual-polarization slot antenna using a compact CPW feeding structure," *IEEE Antennas Wireless Propag. Lett.*, Vol. 9, 191–194, 2010.

9. Huang, J., "A technique for an array to generate circular polarization with linearly polarized elements," *IEEE Trans. Antennas Propag.*, Vol. 34, 1113–1124, 1986.

10. Chiba, T., Y. Suzuki, and N. Miyano, "Suppression of higher modes and cross polarized component for microstrip antennas," *IEEE Antennas Propagation Soc. Int. Symp. Dig.*, 285–288, 1982.

11. Wu, C.-J., I.-F. Chen, and C.-M. Peng, "A dual polarization bow-tie slot antenna for broadband communications," *PIERS Proceedings*, 217–221, Marrakesh, Morocco, Mar. 20–23, 2011.

12. Xie, J.-J., Y.-Z. Yin, J. Ren, and T. Wang, "A wideband dual-polarized patch antenna with electric probe and magnetic loop feeds," *Progress In Electromagnetics Research*, Vol. 132, 499–515, 2012.

13. Guo, Y. X., K. W. Khoo, and L. C. Ong, "Wideband dual-polarized patch antenna with broadband baluns," *IEEE Trans. Antennas Propag.*, Vol. 55, No. 1, 78–83, 2007.

14. Paryani, R. C., P. F. Wahid, and N. Behdad, "A wideband, dual-polarized, substrate-integrated cavity-backed slot antenna," *IEEE Antennas Wireless Propag. Lett.*, Vol. 9, 645–648, 2010.

15. Xie, J.-J., X.-S. Ren, Y.-Z. Yin, and J. Ren, "Dual-polarised patch antenna with wide bandwidth using electromagnetic feeds," *Electronics Lett.*, Vol. 48, No. 22, 1385–1386, 2012.

16. Siu, L., H. Wong, and K. M. Luk, "A dual-polarized magneto-electric dipole with dielectric loading," *IEEE Trans. Antennas Propag.*, Vol. 57, No. 7, 616–623, 2009.

17. Guo, Y. X., K. M. Luk, and K. F. Lee, "Broadband dual polarization patch element for cellar-phone base stations," *IEEE Trans. Antennas Propag.*, Vol. 50, No. 2, 251–253, 2002.